EXPERIMENTAL IDENTIFICATION OF A NON-LINEAR BEAM, CONDITIONED REVERSE PATH METHOD

G. Kerschen, V. Lenaerts and J.-C. Golinval

Université de Liège, LTAS – Vibrations et identification des structures,
Chemin des chevreuils, 1 (Bât. B52), 4000 Liège, Belgium
Email : g.kerschen@ulg.ac.be

SUMMARY: A new spectral approach for identification of multi-degree-of-freedom non-linear systems, called the conditioned reverse path method, has recently been introduced. The key idea of this method is to eliminate the distortions caused by the presence of non-linearities in frequency response functions. Conditioned frequency responses are then computed and yield the underlying linear properties without influence of non-linearities. The non-linear coefficient is estimated in a second step.

The aim of the paper is twofold. Firstly, the conditioned reverse path method is described in details together with the spectral conditioning techniques. Secondly, the ability of this technique to identify the behaviour of an experimental cantilever beam with a geometrical non-linearity is tested.

KEYWORDS: non-linear system identification – conditioned reverse path – geometrical non-linearity – experimental application.

INTRODUCTION

The last twenty years have witnessed impressive progress in non-linear structural dynamics. The identification of non-linear systems began in 1979 with the study of single-degree-of-freedom (s.d.o.f.) systems [1]. Since then, techniques which can consider multi-degree-of-freedom (m.d.o.f.) systems were introduced, i.e. the Hilbert transform [2], NARMAX models [3-4] and Volterra series [5]. However, it appeared quickly that these techniques are not suitable for systems with high modal density. For a detailed review of the past years, the reader is referred to [6]. Recently, progress in the analysis of m.d.o.f. systems has been realised. This progress can be attributed to a confluence of new methods of analysis and to the expansion in computer processor power.

The non-linear identification through feedback of the outputs (NIFO) [7] is a frequency-domain formulation and treats non-linearities as internal feedback forces in the underlying linear system. The key advantage of the method lies in the fact that the frequency response

functions of the underlying linear system as well as the non-linearities are estimated in a single step. This is done in a least-squares system of equations through averaging.

Proper orthogonal decomposition is emerging as an efficient method in the field of structural dynamics to solve both direct and inverse problems [8-10]. Particularly, it can be exploited for identification and model updating of non-linear systems [11]. The procedure is based on the solution of an optimisation problem which consists in minimising the difference between the bi-orthogonal decompositions of the measured and simulated data respectively.

The conditioned reverse path formulation [12] extends the application of the reverse path algorithm to systems characterised by non-linearities away from the location of the applied force. This technique has been developed by generalising the concepts introduced by Bendat [13-14]. The presence of non-linearities introduces distortions in the frequency response functions computed by the "H_1" and "H_2" methods. In the conditioned reverse path, "conditioned" frequency responses are estimated and yield the underlying linear properties without influence of non-linearities. The non-linear coefficients are identified in a second step.

In this paper, the theoretical background of the conditioned reverse path method is first recalled, together with the spectral conditioning techniques. Then the ability of this technique to identify the behaviour of an experimental cantilever beam with a geometrical non-linearity is tested.

CONDITIONED REVERSE PATH (CRP) METHOD

For the sake of clarity, all the subsequent developments consider a system with a single non-linearity. However, it is worth pointing out that the generalisation to multiple non-linearities is straightforward [12].

The equations of motion of a system with a single non-linearity takes the form

$$\mathbf{M}\ddot{\mathbf{x}}(t) + \mathbf{C}\dot{\mathbf{x}}(t) + \mathbf{K}\mathbf{x}(t) + \mathbf{A}\mathbf{y}(t) = \mathbf{f}(t) \tag{1}$$

where $\mathbf{y}(t)$ is a non-linear function vector often represented as a function of relative displacements. In the frequency domain, equation (1) becomes

$$\mathbf{B}(w)\mathbf{X}(w) + \mathbf{A}\mathbf{Y}(w) = \mathbf{F}(w) \tag{2}$$

where $\mathbf{B}(w) = \mathbf{H}^{-1}(w) = -w^2\mathbf{M} + iw\mathbf{C} + \mathbf{K}$ is the linear dynamic stiffness matrix. A reverse path model is constructed by imposing the applied force to be the output and the measured responses to be the inputs. This is illustrated in Fig. 1.

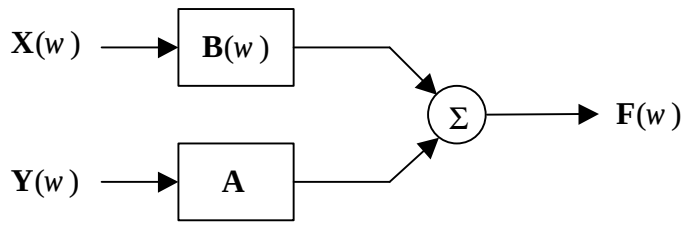

Fig. 1: Reverse path Model

Estimation of the underlying linear system properties

The key idea of the CRP method is the separation of the non-linear part of the system response from the linear part and the construction of uncorrelated response components in the frequency domain. The spectra of the measured responses $\mathbf{X}$ can be decomposed into a component which is correlated with the spectrum of the non-linear vector $\mathbf{Y}$, denoted by $\mathbf{X}_{(+1)}$, through a frequency response matrix $\mathbf{L}_{1X}$, and a component which is uncorrelated with the spectrum of the non-linear vector, denoted by $\mathbf{X}_{(-1)}$ (see Fig. 2). In other words, $\mathbf{X}_{(-1)}$ is the linear spectral component of the response.

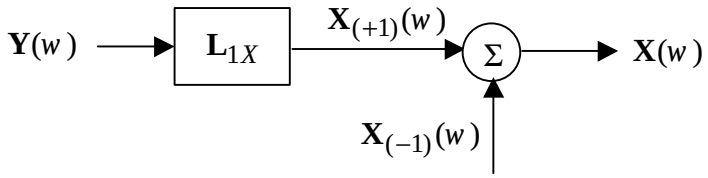

Fig. 2: Decomposition of the spectra of the measured responses

Thus, Fig. 1 may be replaced by Fig. 3 where the inputs $\mathbf{X}_{(-1)}$ and $\mathbf{Y}$ are uncorrelated. The path between $\mathbf{Y}$ and $\mathbf{F}_{(+1)}$ is the frequency response matrix $\mathbf{L}_{1F}$ while the path between $\mathbf{X}_{(-1)}$ and $\mathbf{F}_{(-1)}$ is the linear dynamic stiffness matrix $\mathbf{B}$:

$$\mathbf{Y}(w)\,\mathbf{L}_{1F}(w) = \mathbf{F}_{(+1)}(w) \tag{3}$$

$$\mathbf{X}_{(-1)}(w)\,\mathbf{B}(w) = \mathbf{F}_{(-1)}(w) \tag{4}$$

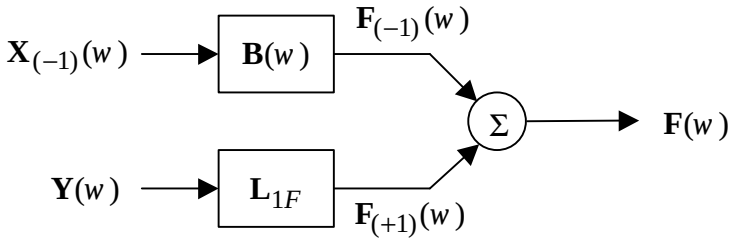

Fig. 3: Reverse path model with uncorrelated inputs

By transposing equation (4), by multiplying it by the complex conjugate of $\mathbf{X}$, i.e. $\mathbf{X}^*$, by taking the expectation and by multiplying by $2/T$, the underlying linear system may be identified without corruption from the non-linear term

$$\mathbf{G}_{XF(-1)} = \frac{2}{T}E[\mathbf{X}^*\mathbf{F}_{(-1)}^T] = \frac{2}{T}E[\mathbf{X}^*(\mathbf{B}\mathbf{X}_{(-1)})^T] = \frac{2}{T}E[\mathbf{X}^*\mathbf{X}_{(-1)}^T\mathbf{B}^T] = \mathbf{G}_{XX(-1)}\mathbf{B}^T \tag{5}$$

where $\mathbf{G}_{XF(-1)}$ and $\mathbf{G}_{XX(-1)}$ are conditioned power spectral density matrices. From equation (5), the dynamic compliance matrix $\mathbf{H}$ can be estimated

$$H_{c2} : \mathbf{H}^T = \mathbf{G}_{XF(-1)}^{-1} \mathbf{G}_{XX(-1)} \tag{6}$$

This expression is known as the conditioned H_{c2} estimate. If relation (4) is multiplied by the complex conjugate of $\mathbf{F}$ instead of $\mathbf{X}$, the conditioned H_{c1} estimate is obtained

$$H_{c1} : \mathbf{H}^T = \mathbf{G}_{FF(-1)}^{-1} \mathbf{G}_{FX(-1)} \tag{7}$$

It should be noted that if the number of excitations is smaller than the number of measured responses, then matrix $\mathbf{G}_{XF(-1)}$ is not square. In this, case, the pseudo-inverse of this matrix is performed rather than the inverse.

Estimation of the non-linear coefficient

Once the linear dynamic compliance $\mathbf{H}$ has been identified, the non-linear coefficient $\mathbf{A}$ may be computed. Transposing the equations of motion in the frequency domain (2), multiplying these by the complex conjugate of $\mathbf{Y}$, taking the expectation and finally multiplying by $2/T$ yields

$$\mathbf{G}_{1X} \mathbf{B}^T + \mathbf{G}_{11} \mathbf{A}^T = \mathbf{G}_{1F} \tag{8}$$

where $\mathbf{G}_{1X}$ is the cross spectral density matrix between the non-linear term $\mathbf{Y}$ and the measured responses ;

$\mathbf{G}_{11}$ is the power spectral density matrix of the non-linear term $\mathbf{Y}$;

$\mathbf{G}_{1F}$ is the cross spectral density matrix between the non-linear term $\mathbf{Y}$ and the measured forces.

If the non-linear coefficient is isolated in equation (8), this equation becomes

$$\mathbf{A}^T = \mathbf{G}_{11}^{-1} (\mathbf{G}_{1F} - \mathbf{G}_{1X} \mathbf{B}^T) \tag{9}$$

In practice, the knowledge of the linear dynamic compliance is preferred. Accordingly, equation (9) is rewritten in a more suitable form

$$\mathbf{A}^T \mathbf{H}^T = \mathbf{G}_{11}^{-1} (\mathbf{G}_{1F} \mathbf{H}^T - \mathbf{G}_{1X}) \tag{10}$$

If excitations are not applied at every response locations, only the columns corresponding to the degree-of-freedom where excitations are applied are determined. However, by taking advantage of the reciprocity principle, the non-linear coefficient $\mathbf{A}$ may be estimated. Let illustrate this on a three degree-of-freedom system with a non-linear term between the second and third degree-of-freedom and with a force applied on the first degree-of-freedom. In this case, equation (10) becomes at each frequency

$$[0 \quad a \quad -a]\begin{bmatrix} H_{11} & H_{21} & H_{31} \\ \times & \times & \times \\ \times & \times & \times \end{bmatrix} =$$

$$G_{11}^{-1}([G_{1F} \quad 0 \quad 0]\begin{bmatrix} H_{11} & H_{21} & H_{31} \\ \times & \times & \times \\ \times & \times & \times \end{bmatrix} - [G_{1X_1} \quad G_{1X_2} \quad G_{1X_3}]) \qquad (11)$$

Expression (11) clearly illustrates that the non-linear coefficient can not be identified since it is multiplied by unknown quantities. However, due to the reciprocity principle, $H_{12} = H_{21}$ and $H_{13} = H_{31}$, and equation (11) is rewritten in the following form

$$[0 \quad a \quad -a]\begin{bmatrix} H_{11} & H_{21} & H_{31} \\ H_{12} & \times & \times \\ H_{13} & \times & \times \end{bmatrix} =$$

$$G_{11}^{-1}([G_{1F} \quad 0 \quad 0]\begin{bmatrix} H_{11} & H_{21} & H_{31} \\ H_{12} & \times & \times \\ H_{13} & \times & \times \end{bmatrix} - [G_{1X_1} \quad G_{1X_2} \quad G_{1X_3}]) \qquad (12)$$

and,

$$a = \frac{G_{1F}H_{11} - G_{1X_1}}{G_{11}(H_{12} - H_{13})} \qquad (13)$$

It is worth pointing out that the non-linear coefficient is frequency dependent. By taking the spectral mean, the actual value of the coefficient should be retrieved.

Conditioned power spectral density matrices

It remains now to indicate how conditioned power spectral density matrices like $\mathbf{G}_{XF(-1)}$ are computed. For the sake of simplicity, only the final formulae are described here. It can be shown [15] that

$$\mathbf{G}_{ij(-1:r)} = \mathbf{G}_{ij(-1:r-1)} - \mathbf{G}_{ir(-1:r-1)}\mathbf{L}_{rj}^{T} \qquad (14)$$

with $$\mathbf{L}_{ji}^{T} = \mathbf{G}_{jj(-1:j-1)}^{-1}\mathbf{G}_{ji(-1:j-1)} \qquad (15)$$

Since the developments are underlined for a single non-linearity, the two latter equations are written in a simpler manner

$$\mathbf{G}_{ij(-1)} = \mathbf{G}_{ij} - \mathbf{G}_{i1}\mathbf{L}_{1j}^{T} \qquad (16)$$

with $$\mathbf{L}_{1j}^{T} = \mathbf{G}_{11}^{-1}\mathbf{G}_{1j} \qquad (17)$$

DESCRIPTION OF THE BENCHMARK

The benchmark is similar to the one proposed by the Ecole Centrale de Lyon (France) in the framework of COST Action F3 working group on “Identification of non-linear systems” [16]. This experimental application involves a clamped beam with a thin part at the end of the beam (see Fig. 4).

Seven accelerometers which span regularly the beam are used to measure the response and a displacement sensor is located at the end of the beam. The structure is excited near the clamping (see Fig. 4) and the force is a white-noise sequence band-limited in the 0-500 Hz range. Different excitation levels are considered in the 0.3-21 N rms range.

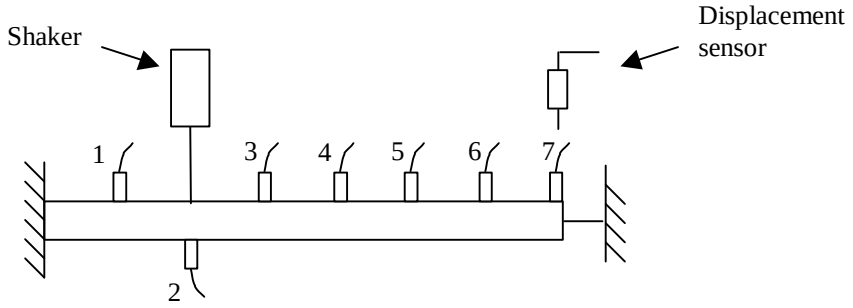

Fig. 4: Tested structure

The frequency response functions (FRFs) are estimated using the H_2 method. Fig. 5 illustrates the magnitude of H_{72} for the 0.3 N rms and 21 N rms levels. As can be seen in this figure, distortions appear in the FRFs when the excitation level increases. This is confirmed by the ordinary coherence functions $\gamma^2_{X_7F}$ (Fig. 6). Accordingly, if the structure may be assumed to be linear for the lowest excitation level, it is no more the case for higher levels. Indeed, if the excitation level is increased, the thin part tends to be excited in large deflection and a geometrical non-linearity is activated.

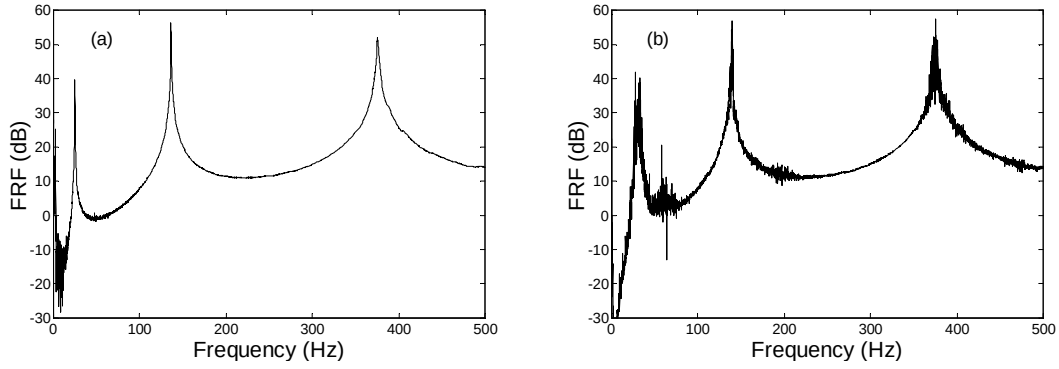

Fig. 5: Magnitude of H_{72} (H_2 estimate). (a) 0.3 N rms ; (b) 21 N rms.

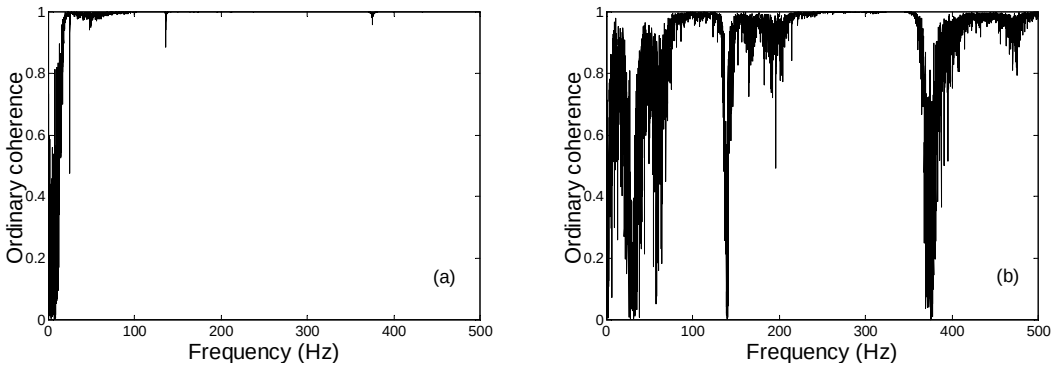

Fig. 6: Ordinary coherence functions $\gamma^2_{X_7F}$. (a) 0.3 N rms ; (b) 21 N rms.

The natural frequencies were also estimated in the 0-500 Hz range using the least squares complex exponential (LSCE) method [17]. Table 1 gives the natural frequencies identified for the different excitation levels. It can be noticed that the first two natural frequencies are shifted towards higher frequencies when the excitation level is increased. This is due to the stiffening effect of the thin part. The third natural frequency does not seem to be affected by the presence of the non-linearity.

Table 1: Estimated natural frequencies (H_2 estimate)

	0.3 N rms	8 N rms	16 N rms	21 N rms
First natural frequency (Hz)	25.00	25.97	28.34	30.44
Second natural frequency (Hz)	136.46	136.65	137.78	139.23
Third natural frequency (Hz)	375.54	375.27	374.43	374.86

RESULTS OF THE IDENTIFICATION

Model selection

The first step in the identification procedure is the selection of a suitable model. To this aim, the cumulative coherence function γ^2_{Mi} may be exploited [18-19]

$$\gamma^2_{Mi}(w) = \gamma^2_{X_iF(-1:n)}(w) + \gamma^2_{YF}(w), \quad i = 1,...,7 \tag{18}$$

where $\gamma^2_{X_iF(-1:n)}(w) = \dfrac{\left|G_{X_iF(-1:n)}(w)\right|^2}{G_{X_iX_i(-1:n)}(w)G_{FF}(w)}$ and $\gamma^2_{YF}(w) = \sum_{j=1}^{n} \gamma^2_{jF(-1:j-1)}(w)$

The cumulative coherence functions are scalar values between 0 and 1 at each frequency and may be considered as a measure of the accuracy of the entire model.

Due to the presence of a second harmonic of the first mode in the FRF (see Fig. 5b), a grounded quadratic spring at the end of the beam (location 7) was introduced in the model. To take the stiffening effect of the thin part into account, a non-linearity of type $|x|^a \, sign(x)$ was added to the quadratic spring. Finally, the non-linearity is modelled as

$$f(x) = A|x|^a \, sign(x) + Bx^2 \tag{19}$$

where x is the displacement at the end of the beam. Exponent a is determined by seeking the maximum value for the spectral mean of the averaged cumulative coherence of all the sensors

$$accuracy = \frac{1}{N} \sum_{w=10}^{500} \left(\frac{1}{7} \sum_{i=1}^{7} \gamma^2_{Mi}(w) \right) \tag{20}$$

where N is the number of frequencies considered between 10 and 500 Hz. The maximum value is found for $a = 3$ and is equal to 0.9834 (21 N rms).

Estimation of the FRFs of the underlying linear system

The H_{c2} estimate (6) is used to compute the FRFs of the underlying linear system. Fig. 7 illustrates the magnitude of $H_{72}^{[c2]}$ together with the cumulative coherence γ^2_{M7} (21 N rms level). Aside from a few minor drops, the cumulative coherence is unity indicating that the model is quite accurate.

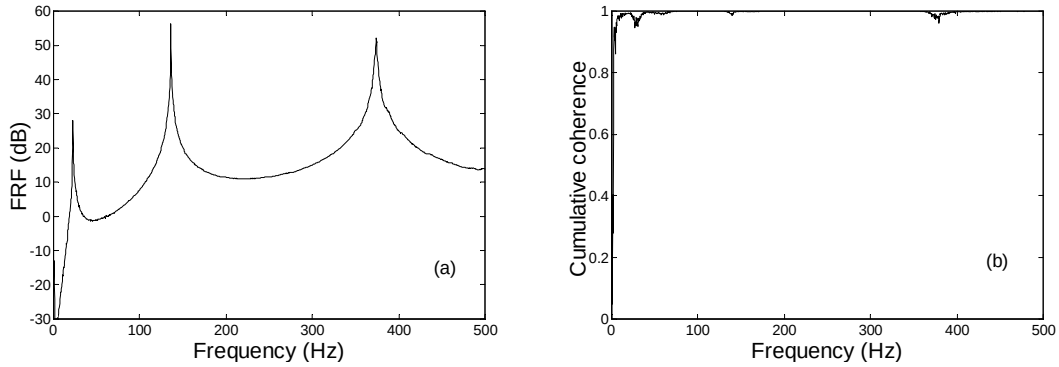

Fig. 7: 21 N rms level. (a) Magnitude of $H_{72}^{[c2]}$; (b) Cumulative coherence γ^2_{M7}.

Fig. 8 represents the comparison between the true FRF and the FRFs obtained using the H_{c2} and H_2 estimates for the first two resonances (21 N rms level). It can clearly be seen that the H_{c2} estimate is closer to the true FRF while the H_2 estimate is contaminated by the presence of the non-linearity.

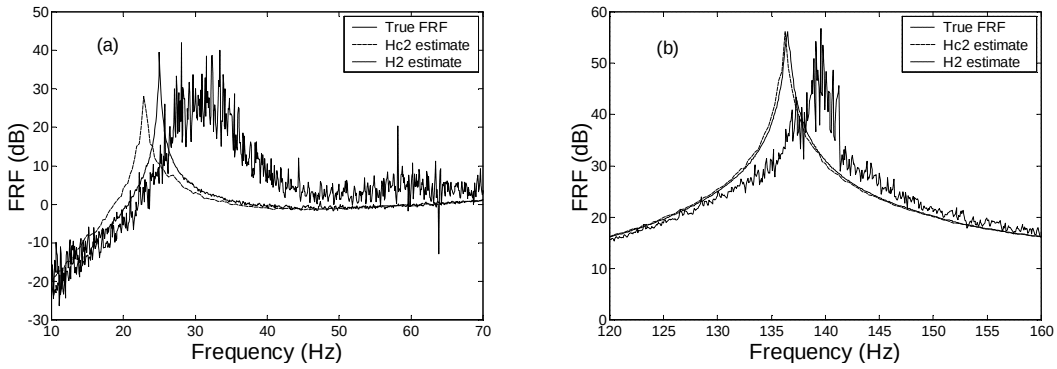

Fig. 8: Comparison of the true FRF with the H_{c2} and H_2 estimates (21 N rms level). (a) First resonance ; (b) Second resonance.

Again, the natural frequencies were estimated from the H_{c2} estimates in the 0-500 Hz range using LSCE method. Table 2 gives the natural frequencies identified for the different excitation levels. The comparison between Tables 1 and 2 shows that

- the natural frequency of the first mode (H_{c2} estimate) tends to decrease when the excitation level is increased. Nevertheless, the H_{c2} estimate is closer to the actual value than the H_2 estimate.
- the natural frequency of the second mode (H_{c2} estimate) remains constant and is almost equal to the actual value. For the H_2 estimate, the natural frequency of this mode is shifted towards higher frequencies when the excitation level is increased.

Table 2: Estimated natural frequencies (H_{c2} estimate)

	0.3 N rms	8 N rms	16 N rms	21 N rms
First natural frequency (Hz)	25.00	24.49	23.35	23.11
Second natural frequency (Hz)	136.46	136.17	136.14	136.24
Third natural frequency (Hz)	375.54	374.55	373.88	373.71

Estimation of the non-linear coefficient

Once the FRFs of the underlying linear system have been estimated, the non-linear coefficients may then be evaluated. Fig. 9 displays the real part of the non-linear coefficients A and B (19). As pointed out before, the coefficients are frequency dependent and a spectral mean has to be performed to have an estimation of the coefficients. However, it can be noticed that the quadratic non-linearity only improves the FRFs around the second harmonic. This is the reason why the spectral mean of the quadratic coefficient is realised between 50 and 80 Hz.

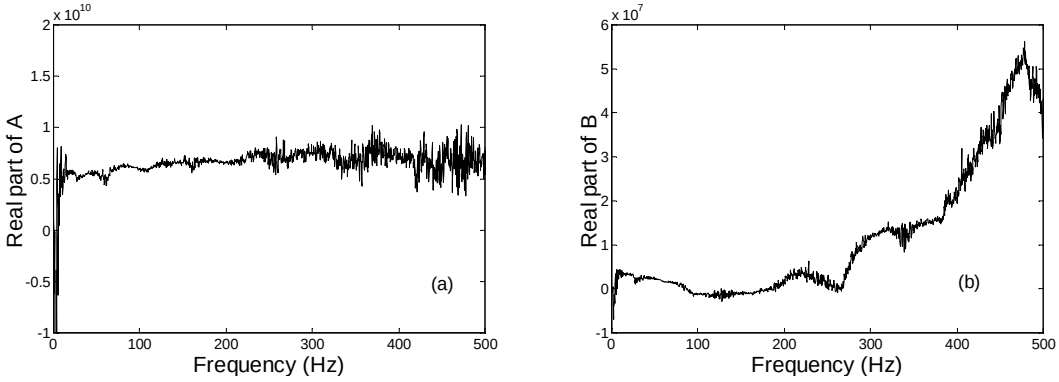

Fig. 9: Real part of the non-linear coefficients (21 N rms level). (a) A ; (b) B.

Table 3 gives the spectral mean of coefficients A and B for the 8, 16 and 21 N rms levels. Firstly, it can be seen that the imaginary part of the coefficients, without any physical meaning, is several orders of magnitude below the real part. Secondly, the real part of the coefficients is quite stable while the excitation level goes from 8 N rms up to 21 N rms.

Table 3: Spectral mean of the non-linear coefficients

	A (10-500 Hz) ($N/m^{3.5}$)	B(50-80 Hz) (N/m^2)
8 N rms	$6.43\ 10^9 + i\ 1.96\ 10^7$	$2.60\ 10^6 + i\ 1.24\ 10^3$
16 N rms	$6.68\ 10^9 + i\ 1.29\ 10^8$	$1.83\ 10^6 - i\ 2.77\ 10^4$
21 N rms	$6.66\ 10^9 + i\ 1.59\ 10^8$	$1.81\ 10^6 + i\ 2.95\ 10^4$

CONCLUSIONS

The aim of this paper was to apply the CRP method to a non-linear beam. The non-linearity was realised by a thin beam excited in large deflection. On the one hand, the H_2 estimate was unable to recover the linear dynamic compliance functions of a multi-degree-of-freedom non-linear system. On the other hand, the H_{c2} estimate, proposed by the CRP method, allowed to reduce significantly the distortions introduced by the non-linearities. Moreover, the method leads to the estimation of reliable non-linear coefficients.

The key advantage of the method is its ability to deal with multi-degree-of-freedom non-linear systems. In this context, it appears as a useful method to be employed on more complex non-linear structures.

ACKNOWLEDGEMENTS

Mr. Kerschen is supported by a grant from the Belgian National Fund for Scientific Research which is gratefully acknowledged. This work also presents research results of the Belgian programme on Inter-University Poles of Attraction initiated by the Belgian state, Prime Minister's office, Science Policy Programming. The scientific responsibility is assumed by its authors.

REFERENCES

1. Masri, S.F., Caughey, T.K., "A Nonparametric Identification Technique for Nonlinear Dynamic Problems ", Journal of Applied Mechanics **46**, 1979, pp. 433-447.
2. Simon, M., Tomlinson, G.R., "Application of the Hilbert Transform in Modal Analysis of Linear and Non-linear Structures", Journal of Sound and Vibration **90**, 1984, pp. 275-282.
3. Leontaritis, I.J., Billings, S.A., "Input-Output Parametric Models for Nonlinear Systems, Part I: Deterministic Nonlinear Systems", International Journal of Control **41**, 1985, pp. 303-328.
4. Leontaritis, I.J., Billings, S.A., "Input-Output Parametric Models for Nonlinear Systems, Part II: Stochastic Nonlinear Systems", International Journal of Control **41**, 1985, pp. 329-344.
5. Gifford, S.J., Tomlinson, G.R., "Recent Advances in the Application of Functional Series to Non-linear Structures", Journal of Sound and Vibration **135**, 1989, pp. 289-317.
6. Worden, K., "Nonlinearity in Structural Dynamics : the Last Ten Years", European COST F3 Conference on System Identification and Structural Health Monitoring, Proceedings of the Conference held in Madrid, 2000, pp. 29-52.
7. Adams, D.E., Allemang, R.J., "A Frequency Domain Method for Estimating the Parameters of a Non-linear Structural Dynamic Model through Feedback", Mechanical Systems and Signal Processing **14**(4), 2000, pp. 637-656.
8. Cusumano, J.P., Sharkady, M.T., Kimble, B.W., "Spatial Coherence Measurements of a Chaotic Flexible-Beam Impact Oscillator", Aerospace Structures: Nonlinear Dynamics and System Response, ASME AD-Vol. **33**, 1993, pp. 13-22.
9. Kappagantu, R., Feeny, B.F., "An Optimal Model Reduction of a System with Frictional Excitation", Journal of Sound and Vibration **224**(5), 1999, pp. 863-877.
10. Azeez, M.F.A., Vakakis, A.F. "Proper Orthogonal Decomposition of a Class of Vibroimpact Oscillations", Journal of Sound and Vibration **240**(5), 2001, pp. 859-889.
11. Lenaerts, V., Kerschen, G., Golinval, J.C., "Proper Orthogonal Decomposition for Model Updating of Non-linear Mechanical Systems", Mechanical Systems and Signal Processing **15**(1), 2000, pp. 31-43.
12. Richards, C.M., Singh, R., "Identification of Multi-degree-of-freedom Non-linear Systems under Random Excitations by the Reverse Path spectral Method", Journal of Sound and Vibration **213**(4), 1998, pp. 673-708.
13. Bendat, J.S., "Nonlinear System Analysis and Identification from Random Data", New York: John Wiley & Sons, Inc, 1990.
14. Bendat, J.S., "Spectral Techniques for Nonlinear System Analysis and Identification", Shock and Vibration **1**, 1993, pp. 21-31.
15. Bendat, J.S., "Random Data: Analysis and Measurement Procedures", New York: John Wiley- Interscience, second edition, 1986.
16. Web-Site, http://www.ulg.ac.be/ltas-vis/costf3/costf3.html
17. Ewins, D.J., "Modal Testing: Theory, Practice and Application", Research Studies Press LTD, Second Edition, 2000.
18. Richards, C.M., Singh, R., "Feasibility of Identifying Non-linear Vibratory Systems Consisting of Unknown Polynomial Forms", Journal of Sound and Vibration **220**(3), 1999, pp. 413-450.
19. Marchesiello, S., Garibaldi, L., Wright, J.R., Cooper, J.E., "Applications of the Conditioned Reverse Path Method to Multi-degree-of-freedom Non-linear Systems", European COST F3 Conference on System Identification and Structural Health Monitoring, Proceedings of the Conference held in Madrid, 2000, pp. 429-438.